

Influence of Ionic Association, Transport Properties, and Solvation on the Catalytic Hydrogenation of 1,3-Cyclohexadiene in Ionic Liquids

Ajda Podgoršek,[†] Gorka Salas,[‡] Paul S. Campbell,[‡] Catherine C. Santini,^{*,‡} Agílio A. H. Pádua,^{†,§} Margarida F. Costa Gomes,^{*,†,§} Bernard Fenet,^{||} and Yves Chauvin[‡]

[†]CNRS, Laboratoire de Thermodynamique et Interactions Moléculaires, UMR 6272, 24 avenue des Landais, BP 80026, 63171 Aubière, France

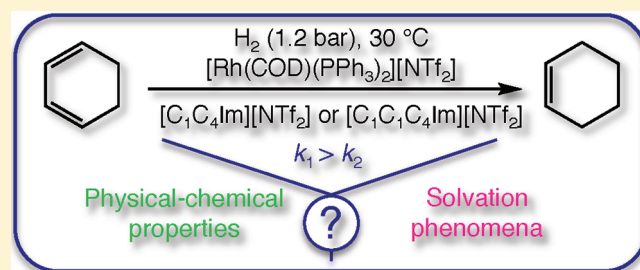
[‡]Université de Lyon, Institut de Chimie de Lyon, UMR 5265 CNRS, Université de Lyon 1-ESCE Lyon, C2P2, Equipe Chimie Organométallique de Surface, ESCPE 43 Boulevard du 11 Novembre 1918, F-69616 Villeurbanne, France

[§]Clermont Université, Université Blaise Pascal, Clermont-Ferrand, France

^{||}Centre Commun de RMN, UCB Lyon 1 - ESCPE Lyon, 43 Boulevard du 11 Novembre 1918, F-69616 Villeurbanne Cedex, France

S Supporting Information

ABSTRACT: The influence of the nature of two different ionic liquids, namely 1-butyl-3-methylimidazolium bis(trifluoromethylsulfonyl)imide, $[C_1C_4Im][NTf_2]$, and 1-butyl-2,3-dimethylimidazolium bis(trifluoromethylsulfonyl)imide, $[C_1C_1C_4Im][NTf_2]$, on the catalytic hydrogenation of 1,3-cyclohexadiene with $[Rh(COD)(PPh_3)_2][NTf_2]$ (COD=1,5-cyclooctadiene) was studied. Initially, the effect of different concentrations of 1,3-cyclohexadiene on the molecular interactions and on the structure in two ionic liquids was investigated by NMR and by molecular dynamic simulations. It was found that in both ionic liquids 1,3-cyclohexadiene is solvated preferentially in the lipophilic regions. Furthermore, the higher solubility of 1,3-cyclohexadiene in $[C_1C_4Im][NTf_2]$ and the smaller positive values of the excess molar enthalpy of mixing for the 1,3-cyclohexadiene + $[C_1C_4Im][NTf_2]$ system in comparison with 1,3-cyclohexadiene + $[C_1C_1C_4Im][NTf_2]$ indicate more favorable interactions between 1,3-cyclohexadiene and the $C_1C_4Im^+$ cation than with the $C_1C_1C_4Im^+$ cation. Subsequently, diffusivity and conductivity measurements of the 1,3-cyclohexadiene + ionic liquid mixtures at different compositions allowed a characterization of mass and charge transport in the media and access to the ionicity of ionic liquids in the mixture. From the dependence of the ratio between molar conductivity and the conductivity inferred from NMR diffusion measurements, $\Lambda_{imp}/\Lambda_{NMR}$, on concentration of 1,3-cyclohexadiene in the ionic liquid mixture, it was found that increasing the amount of 1,3-cyclohexadiene leads to a decrease in the ionicity of the medium. Finally, the reactivity of the catalytic hydrogenation of 1,3-cyclohexadiene using $[Rh(COD)(PPh_3)_2][NTf_2]$ performed in $[C_1C_4Im][NTf_2]$ at different compositions of 1,3-cyclohexadiene and in $[C_1C_1C_4Im][NTf_2]$ at one composition was related linearly to the viscosity, hence the reaction rate is determined by the mass transport properties of the media.



1. INTRODUCTION

Ionic liquids (ILs) are up-and-coming solvents for catalysis, with the number of publications in this field growing at an exponential rate.^{1–3} ILs have specific properties that, when they are used as reaction media, may have more important consequences on catalytic processes than traditional solvents.^{4–9} In some catalytic reactions, the difference between ILs and traditional solvents has been related to their chemical role, interfering with the reaction.^{2,10} For example, imidazolium moieties of the cation may be deprotonated in situ and therefore coordinate to metal centers as imidazolylidene-*N*-heterocyclic carbene ligands.^{11–16} Certain ILs themselves exhibit catalytic activity, for instance Friedel–Crafts alkylations and acylations occur readily in these media.^{17,18} In other cases, differences in reactivity have an origin in physical chemistry,^{2,19} resulting from peculiar solvation phenomena in ILs, which are more structured solvents than molecular fluids.^{16,18,23}

Numerous experimental studies, ranging from NMR spectroscopy focusing on through-space NOE interactions,²⁰ through X-ray diffraction,^{21–23} to neutron scattering,^{24,25} provided strong evidence for a local structuring of pure ILs. Neutron scattering experiments found significant charge ordering in the $[C_1C_2Im][NTf_2]$ ionic liquid,^{20,26} even in the liquid state, whereas X-ray diffraction patterns of super-cooled and liquid imidazolium ionic liquids with different chain lengths¹⁸ indicated structural heterogeneities that varied in size with the length of the alkyl chains in the imidazolium cations. A high degree of self-organization of ionic liquids due to the coexistence of charged moieties and hydrophobic alkyl

Received: July 12, 2011

Revised: September 2, 2011

Published: September 12, 2011

chains was also predicted by molecular dynamics simulations.^{27,28}

The presence of persistent microscopic structures such as segregated nonpolar domains and a polar network influences the way solutes are solvated in ionic liquids.^{29,30} Indeed, radial distribution functions from molecular simulation show that nonpolar solutes dissolve in nonpolar domains, polar solvents interact strongly with polar regions, and amphiphilic molecules such as alcohols have more complex behavior.³¹ However, polarity is not the only relevant property since ionic liquids can exhibit specific interactions, i.e., cation– π interactions between the ionic moieties and the solute, as evidenced by X-ray diffraction of benzene + [C₁C₂Im][NTf₂] mixtures at various compositions.³² Similarly, by combining ROESY NMR and molecular simulation such interactions were shown to be present in the mixtures of toluene with the trialkylimidazolium IL - [C₁C₁C₄Im][NTf₂].²⁶ Contrarily, in the dialkylimidazolium IL, [C₁C₄Im][NTf₂], π -cation interactions are inhibited by the strong H-bond between anion and cation due to the relatively acidic hydrogen on the C₂ position of the imidazolium cation.³² Another NMR study provided supporting evidence that the nature of the IL and its interactions are crucial in determining the solvation environment of thiophene in mixtures with ILs.³³ All these specific interactions may have an effect on reactions depending on the substrate involved in a chemical process.

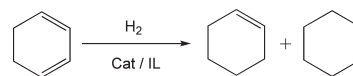
Finally, properties such as density and viscosity have higher values for ionic liquids than for most traditional solvents and thus play more important roles in reaction kinetics by affecting the diffusion of molecules.^{34,35} Viscosity varies greatly with the nature of the IL, and although related to the strength of cation–anion association, it is a physical property that is difficult to predict.^{36,37}

Recently, we have reported how the difference of the activity and the selectivity of the hydrogenation of 1,3-cyclohexadiene, CYD (Scheme 1), in [C₁C₄Im][NTf₂] and [C₁C₁C₄Im][NTf₂] depends on the differences in the physical–chemical properties of the catalytic medium and also solvation of the substrate.³⁸ Following these results, the aim of the present work is to extend and deepen the study of the dynamics of different species involved in the catalytic system of hydrogenation of CYD. We have investigated the transport of species in pure [C₁C₄Im][NTf₂] and [C₁C₁C₄Im][NTf₂] and in their mixtures with CYD at different compositions corresponding to mole fractions of $x_{\text{CYD}} = 0.09, 0.17, 0.20, 0.23, 0.29,$ and 0.33 (CYD/IL mole ratios $R = 0.1, 0.2, 0.25, 0.3, 0.4,$ and 0.5). Furthermore, ion association in the medium (ionicity, strength of cation–anion association) and its effect on the catalytic activity and on the rate of the reaction have been evaluated. This information has been assessed through measurement of the density, viscosity, conductivity, and diffusion coefficients (by 2D DOSY NMR) of CYD + IL mixtures.

2. EXPERIMENTAL SECTION

Materials and Methods. 1-Methylimidazole (>99%, Aldrich) and 1,2-dimethylimidazole (>98%, Aldrich) were distilled prior to use. Anhydrous 1,3-cyclohexadiene (99.8%, Aldrich) and 1,3-cyclohexadiene (96%, Acros Organics, stabilized with 50 ppm of 2,6-di-*tert*-butyl-4-methylphenol, BHT), distilled over NaK alloy and stored on zeolites, were used for the reactions and for the physical–chemical measurements, respectively. Bis(trifluoromethylsulfonyl)imide lithium salt (>99%, Solvionic) and [Rh(COD)Cl]₂ (>99%, Strem) were used without further purification.

Scheme 1. Catalytic Hydrogenation of CYD



All other reagents and solvents were commercially available and were used as received. Ionic liquids, synthesized as previously reported,¹⁴ were dried overnight under high vacuum and stored in a glovebox (Jacomex) in order to guarantee anhydrous products.

Density and Viscosity. The mixtures of CYD and ionic liquids at different compositions, expressed in mole fraction $x_{\text{CYD}} = n_{\text{CYD}}/(n_{\text{CYD}} + n_{\text{IL}})$ or in the molar ratio $R = n_{\text{CYD}}/n_{\text{IL}}$, with $x_{\text{CYD}} = R/(R+1)$, were prepared gravimetrically following a procedure already described, including the precautions to minimize vapor headspace.³⁸ The uncertainty of the mole fraction is estimated as ± 0.0001 . The viscosity of the mixtures was measured using a rolling-ball viscometer from Anton Paar, model AMVn equipped with capillary tubes of 3.0 and 1.8 mm in diameter, at 298.15 ± 0.05 K (the uncertainty is the total combined accuracy and precision; the temperature is controlled to within ± 0.005 K). Before starting the measurements, the 3.0 mm diameter capillary tube had been calibrated as a function of temperature and angle of measurement using a standard viscosity oil from Cannon (N35). The capillary with 1.8 mm diameter had been calibrated with water by the manufacturer. The overall uncertainty in viscosity is estimated to be $\pm 2\%$.

The density of the mixtures, necessary to determine the dynamic viscosities, was measured with an Anton Paar vibrating tube densimeter model 512 P at 298.15 ± 0.02 K. The densimeter was calibrated on *n*-heptane, bromobenzene, and 2,4-dichlorotoluene. The overall uncertainty of the density is estimated as $\pm 0.03\%$.

Conductivity. Electrolytic conductivities were measured by the AC impedance bridge technique at 298.15 K using a conductivity cell, as described previously.³⁹ The cell, made of borosilicate glass with two platinum electrodes, was used in a sealed vessel to avoid atmospheric moisture while measuring. The cell was immersed in a thermostatic bath and the temperature was measured using a four-wire platinum resistance thermometer leading to an estimated uncertainty of ± 0.1 K. The cell had been previously calibrated at 298.15 K using a commercial conductivity standard consisting of an aqueous potassium chloride solution (HI 7031, Hanna Instruments, with conductivity $1413 \mu\text{S}/\text{cm}$) from which the constant of the cell was determined to be $K_{\text{cell}} = 104.98 \pm 0.01 \text{ m}^{-1}$. The conductivity cell was carefully cleaned using deionized water and ethanol and dried using a flow of dry nitrogen before the measurements. The mixtures of CYD and ionic liquid at different compositions were prepared gravimetrically. The conductivity cell was then filled with approximately 2.5 mL of the mixture, sealed, and immersed in the thermostatic bath. The electrical resistance, R , was measured at several frequencies ranging from $f = 0.8$ to 5 kHz using a Wayne Kerr Precision Component Analyzer model 6430B. Afterward the resistance at infinite frequency R^∞ was determined by plotting R against $f^{-1/2}$ and extrapolating to 0, leading to the electrical conductivity, $\kappa = K_{\text{cell}}/R^\infty$. The uncertainty in the measurements of κ is estimated to be $\pm 0.05\%$. The molar conductivity $\Lambda = \kappa/c$ was then calculated using the molar concentration of ionic liquid.

NMR Spectroscopy. ¹H and ¹³C solution NMR spectra were recorded on a Bruker DRX 500 instrument at 298 K (nominal)

with a resonance frequency at 500.130 MHz. The solvent used was CD_2Cl_2 , distilled and kept in a rotaflo with molecular sieves. Chemical shifts are reported in ppm (singlet = s, doublet = d, doublet of doublet = dd, and multiplet = m) and were measured relative to residual proton of the solvent to CHDCl_2 for ^1H , and to CD_2Cl_2 for ^{13}C .

Samples with different compositions were prepared by stirring the mixtures of CYD and the corresponding IL for a few hours, as already described.³⁸ The sample was then introduced into a 5 mm NMR tube, in which a capillary tube with CD_2Cl_2 was loaded to avoid any contact between the deuterated solvent and the mixture analyzed. The deuterium in CD_2Cl_2 was used for the external lock of the NMR magnetic field. The composition was further verified by ^1H NMR spectroscopy.

For the pulsed-field-gradient spin echo NMR DOSY (DOSY, Diffusion Order Spectroscopy) experiments, a Bruker sequence ledbpgp2s was implemented for shorter pulse gradients to improve line shape and trapezoidal gradients (the pulse sequences are shown in Figure S1 in the Supporting Information). The diffusion evolution time was 100 ms, the constant amplitude part of the gradient was 3 ms, and the cosine raising and falling parts of gradient were 150 μs . The diffusion space was sampled by 32 linearly spaced gradients.

Molecular Simulation. The microscopic structures of the CYD + IL mixtures studied experimentally were investigated by molecular dynamic simulations using an atomistic force field that describes interactions and conformations.^{40–42} CYD was represented by the Optimized Potential for Liquid Simulations force field in its all-atom explicit version (OPLS-AA).⁴³ ILs were represented by a specifically parametrized force field, compatible with OPLS-AA, in which particular attention was paid to the description of electrostatic charge distributions and torsion energy profiles. Details were given in previous work.³⁸

Molecular dynamics simulations of condensed-phase CYD + $[\text{C}_1\text{C}_4\text{Im}][\text{NTf}_2]$ and CYD + $[\text{C}_1\text{C}_1\text{C}_4\text{Im}][\text{NTf}_2]$ mixtures were performed using the DL_POLY program.⁴⁴ Numbers of cations, anions and CYD molecules varied according to composition (e.g., 182 ion pairs and 18 molecules of CYD for $x_{\text{CYD}} = 0.09$, 192 ion pairs and 64 molecules of CYD for $x_{\text{CYD}} = 0.25$, 128 ion pairs and 64 molecules of CYD for $x_{\text{CYD}} = 0.33$, 111 ion pairs and 89 molecules of CYD for $x_{\text{CYD}} = 0.45$). Initial low-density configurations, with ions and molecules placed at random in periodic cubic boxes, were equilibrated to attain liquid-like densities and structures at 400 K and 1 bar. The complete conditions under which molecular simulations were performed were described in a previous publication.³⁸

Synthesis of the Catalyst. The whole procedure for the synthesis of $[\text{Rh}(\text{COD})(\text{PPh}_3)_2]\text{NTf}_2$, including characterization by ^1H , ^{31}P , and ^{103}Rh NMR and mass spectrometry, was described previously.³⁸

Hydrogenation of 1,3-Cyclohexadiene. The hydrogenation of CYD was carried out at 1.2 atm of H_2 and 303 K. CYD was dissolved under argon in a solution of $[\text{Rh}(\text{COD})(\text{PPh}_3)_2][\text{NTf}_2]$ in one of the ionic liquids, $[\text{C}_1\text{C}_4\text{Im}][\text{NTf}_2]$ or $[\text{C}_1\text{C}_1\text{C}_4\text{Im}][\text{NTf}_2]$, resulting in red homogeneous solutions. The reaction mixture was kept under hydrogen atmosphere (1.2 bar, constant pressure) until 4 mL of acetonitrile were added. The distribution of products in the reaction mixture and the conversion were determined by GC analyses using a HP6890 chromatograph equipped with a FID detector and a cross-linked methyl siloxane column ($L = 30$ m, $\phi_{\text{int}} = 0.32$ mm, film thickness = 0.25 μm) and toluene as an internal standard. The injector and

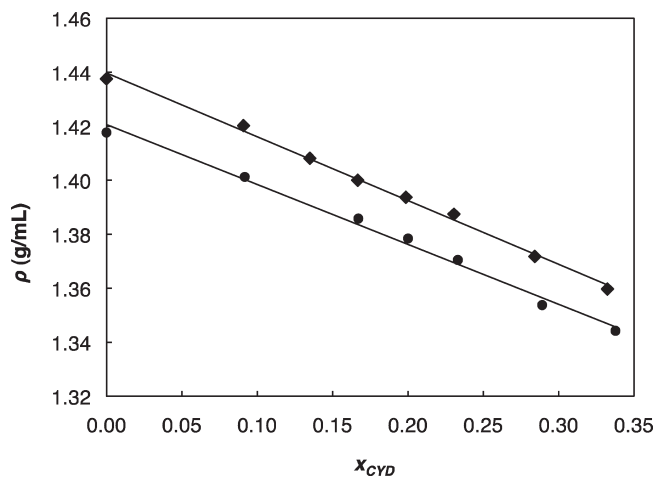


Figure 1. Density of the mixtures CYD + $[\text{C}_1\text{C}_4\text{Im}][\text{NTf}_2]$ (◆) and CYD + $[\text{C}_1\text{C}_1\text{C}_4\text{Im}][\text{NTf}_2]$ (●) as a function of composition. The lines represent functions: $\rho(\text{g/mL}) = -0.2217x_{\text{CYD}} + 1.4206$ (●) and $\rho(\text{g/mL}) = -0.2359x_{\text{CYD}} + 1.4397$ (◆); x_{CYD} is the mole fraction of CYD in the mixture.

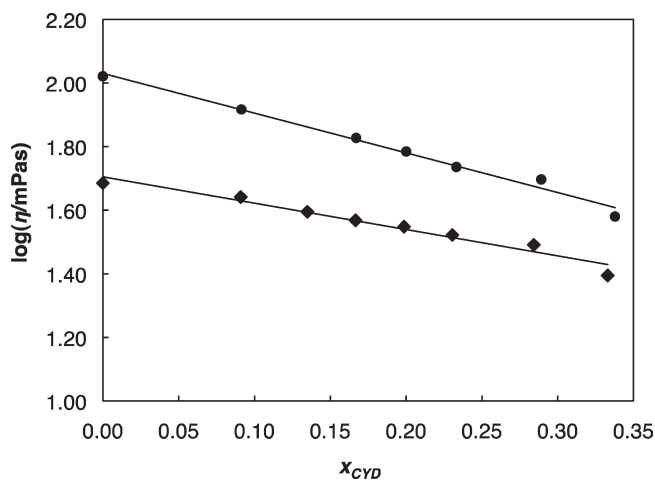


Figure 2. Logarithm of the viscosity of CYD + $[\text{C}_1\text{C}_4\text{Im}][\text{NTf}_2]$ (◆) and CYD + $[\text{C}_1\text{C}_1\text{C}_4\text{Im}][\text{NTf}_2]$ (●) mixtures as a function of composition. The lines represent functions $\log(\eta/\text{mPas}) = -1.2481x_{\text{CYD}} + 2.030$ (●) and $\log(\eta/\text{mPas}) = -0.8281x_{\text{CYD}} + 1.705$ (◆).

detector temperatures were both set to 230 °C. Samples were injected in volumes of 1 μL . The temperature of the column was fixed at 70 °C for 13.5 min, followed by a temperature ramp of 40 °C min^{-1} up to 250 °C.

The experiments to study the effect of stirring and of hydrogen pressure on the reaction were carried out in a multireactor device Thermo Fisher Scientific ATS20000, Integrity 10, allowing simultaneous reactions with well-controlled and different stirring speeds.

3. RESULTS AND DISCUSSION

Density and Viscosity. The density and viscosity of the mixtures of CYD + $[\text{C}_1\text{C}_4\text{Im}][\text{NTf}_2]$ and CYD + $[\text{C}_1\text{C}_1\text{C}_4\text{Im}][\text{NTf}_2]$ as a function of mole fraction were measured at 298.15 K and atmospheric pressure. The results are presented in Table S1 (Supporting Information) and Figures 1 and 2. As already observed,

Scheme 2. Labeling of the Atoms in the Imidazolium Cation and in 1,3-Cyclohexadiene

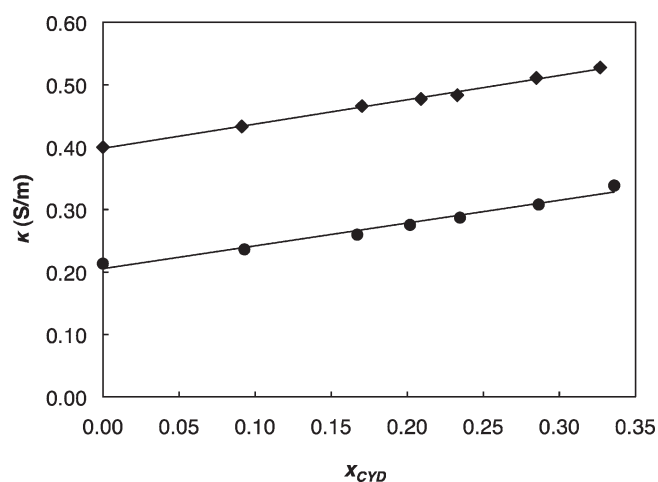
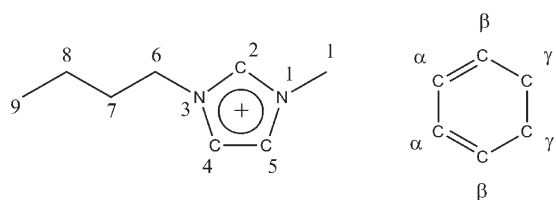


Figure 3. Electrolytic conductivity, κ of the mixtures CYD + $[\text{C}_1\text{C}_4\text{Im}][\text{NTf}_2]$ (\blacklozenge) and CYD + $[\text{C}_1\text{C}_1\text{C}_4\text{Im}][\text{NTf}_2]$ (\bullet) as a function of composition. The lines represent functions: κ (S/m) = $0.3653x_{\text{CYD}} + 0.2053$ (\bullet) and κ (S/m) = $0.388x_{\text{CYD}} + 0.3982$ (\blacklozenge).

the additional methyl group on the imidazolium carbon C_2 in $[\text{C}_1\text{C}_1\text{C}_4\text{Im}][\text{NTf}_2]$ (Scheme 2 for atom labeling) increases the molar volume² and hence lowers molar density of the liquid in comparison with $[\text{C}_1\text{C}_4\text{Im}][\text{NTf}_2]$. The same effect remains in the mixtures with CYD. On the other hand, the viscosity of pure $[\text{C}_1\text{C}_1\text{C}_4\text{Im}][\text{NTf}_2]$ and also of its mixtures with CYD is roughly twice that of $[\text{C}_1\text{C}_4\text{Im}][\text{NTf}_2]$ and of $[\text{C}_1\text{C}_4\text{Im}][\text{NTf}_2]$ + CYD (Figure 2), as already reported.³⁸ However, the decrease in viscosity with concentration for the two systems is slightly different. These results are consistent with the observation that reduction in hydrogen bonding leads to an increase in viscosity for the $\text{C}_1\text{C}_1\text{C}_4\text{Im}^+$ based ionic liquids.³⁶

Conductivity. The electrolytic conductivity of a medium is a measure of the number and mobility of available charge carriers and is of critical importance for electrochemical applications.^{2,45} Although ionic liquids are composed entirely of ions, they are in general significantly less conductive than concentrated aqueous electrolytes.⁴⁶ The lower-than-expected conductivity of ionic liquids can be attributed to the reduction of available charge carriers due to ion pairing or other forms of aggregation.

Table S2 (Supporting Information) and Figure 3 show the electrolytic conductivity, κ , for CYD + $[\text{C}_1\text{C}_4\text{Im}][\text{NTf}_2]$ and CYD + $[\text{C}_1\text{C}_1\text{C}_4\text{Im}][\text{NTf}_2]$ as a function of composition. Pure $[\text{C}_1\text{C}_4\text{Im}][\text{NTf}_2]$ and its mixtures with CYD have higher conductivity than pure $[\text{C}_1\text{C}_1\text{C}_4\text{Im}][\text{NTf}_2]$ and the respective mixtures with CYD. Increasing the cation size leads to lower conductivity, most likely due to the lower mobility of the larger cations, as already observed.⁴⁶ For both mixtures, addition of CYD leads to

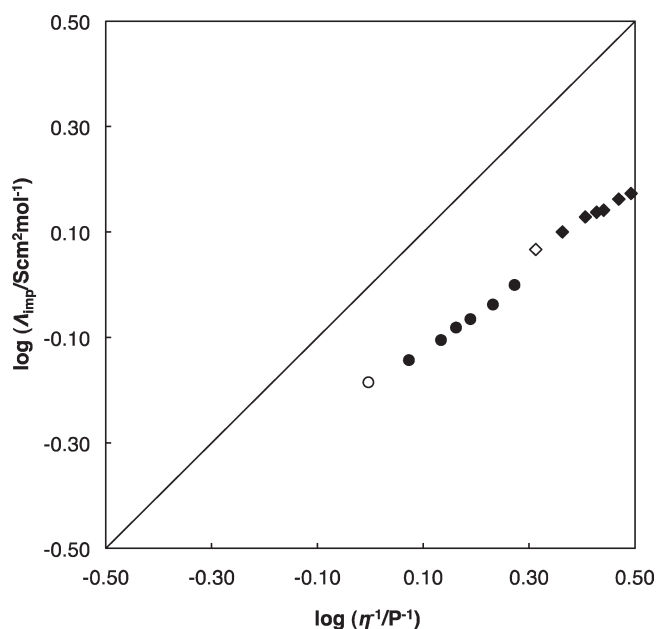


Figure 4. Walden plot, logarithm of molar conductivity against logarithm of reciprocal viscosity, for the mixtures CYD + $[\text{C}_1\text{C}_4\text{Im}][\text{NTf}_2]$ (\blacklozenge) and CYD + $[\text{C}_1\text{C}_1\text{C}_4\text{Im}][\text{NTf}_2]$ (\bullet) as a function of composition. The solid line indicates the ideal line for a completely dissociated strong electrolyte aqueous KCl solution (open symbols for pure ILs, full symbols for mixtures).

increase in electrolytic conductivity, indicating increasing charge mobility.

The observed increase in conductivity with increasing CYD content in the mixtures with ionic liquids can be attributed either to the decreased viscosity and hence increased mobility of charges, or to changes in the structure of the system leading to increasing numbers of charged and mobile species. This information can be accessed through the relationship between conductivity and viscosity in a Walden plot, $\log(\Lambda_{\text{imp}})$ vs $\log(1/\eta)$, where Λ_{imp} is the molar conductivity measured by an impedance method.^{47–49} Plotting the molar conductivity (Λ_{imp} , Figure S2 in the Supporting Information) instead of the absolute conductivity (κ) normalizes to an extent the effects of molar concentration on the conductivity and thus gives a better indication of the number of mobile charge carriers.⁴⁶ The diagonal 1:1 line represents the ideal Walden line, obeyed by 0.01 M aq. KCl, which yields fully dissociated ions with essentially equal mobility. Most ionic liquids fall slightly below the 1:1 line suggesting that ionization (or proton transfer in protic ILs) is not complete in those cases. According to Angell et al.⁴⁸ the vertical distance ΔW of the data points to the reference KCl line is a measure of the deviation of ionic liquid media from electrolytic ideality, i.e., of its (loss of) ionicity. The magnitude of the deviation below the ideal line depends on the structure of ions, since their interactions can strongly influence ionicity, a strong cation–anion association causing poor IL ionicity.⁵⁰ Recently, MacFarlane et al. argued that to compare ionicity between different ionic liquids, one should take into account the radii of the conductive species (ions). For this, an adjusted form of the Walden plot was proposed.⁵¹

Figure 4 shows the Walden plot for the mixtures CYD + $[\text{C}_1\text{C}_4\text{Im}][\text{NTf}_2]$ and CYD + $[\text{C}_1\text{C}_1\text{C}_4\text{Im}][\text{NTf}_2]$ at different compositions, with pure ionic liquids represented by open symbols. From the difference of the deviation of the pure ILs from the

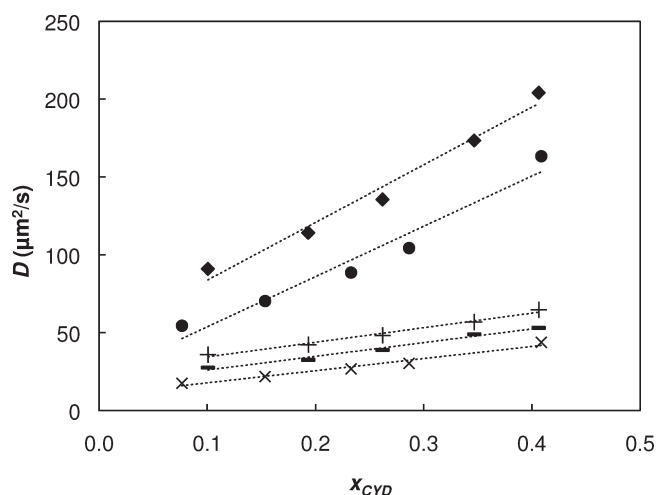


Figure 5. Diffusion coefficients of the cations (+), the anions (−) and CYD (◆) in CYD + [C₁C₄Im][NTf₂]; diffusion coefficients of the cations (×) and CYD³² (●) in CYD + [C₁C₁C₄Im][NTf₂], as a function of CYD mole fraction. Measured by PFG NMR at 298 K.

1:1 line it can be seen that [C₁C₄Im][NTf₂] is less ionic than [C₁C₁C₄Im][NTf₂], indicating that ion pairs in the former case are more associated due to the presence of hydrogen bonds.^{36,52} For both ionic liquids it was found that addition of CYD causes a decrease in ionicity, meaning an alteration in the structure through increased ionic association. In spite of this stronger ionic association, conductivity does increase upon dilution of the IL in CYD, meaning that the effect of diminishing viscosity is dominant, as seen from the Λ_{imp} vs x_{CYD} plot (Figure S2 in the Supporting Information).

DOSY NMR. The behavior of ionic liquids as electrolytes is strongly influenced by the transport properties of their ionic constituents.⁴⁵ These transport properties are related to the mobility of ions and to the degree of ion association (individual ions, ion-pairs, or larger aggregates). The quantity most often used to evaluate the transport properties of electrolytes is the ion diffusion coefficient. In this work the diffusion coefficients were determined by pulse-field-gradient spin-echo (PFGSE) DOSY NMR. Table S3 (Supporting Information) and Figure 5 represent diffusion coefficients of the cation, the anion and the 1,3-cyclohexadiene in CYD + [C₁C₄Im][NTf₂] and CYD + [C₁C₁C₄Im][NTf₂] mixtures at different compositions, with the exception of the diffusion coefficients for NTf₂[−] in [C₁C₁C₄Im][NTf₂], which were not measured. Diffusion coefficients of C₁C₄Im⁺ and NTf₂[−] in the pure [C₁C₄Im][NTf₂] are 3.03×10^{-11} and $2.22 \times 10^{-11} \text{ m}^2 \text{ s}^{-1}$, respectively (obtained from extrapolation of linearly fitted data to $x_{\text{CYD}} = 0$), which is in a good agreement with the data reported in the literature:⁵³ 3.4×10^{-11} and $2.6 \times 10^{-11} \text{ m}^2 \text{ s}^{-1}$, respectively. On the other hand, the diffusion of the cation in pure [C₁C₁C₄Im][NTf₂], $1.38 \times 10^{-11} \text{ m}^2 \text{ s}^{-1}$, is slower than that of the cation in pure [C₁C₄Im][NTf₂], which can be ascribed to higher viscosity of the former IL. In general, the C₁C₄Im⁺ cation has higher diffusion coefficient than the anion, even though the cationic radius is larger.⁵⁴ This is mainly attributed to the planar structure of C₁C₄Im⁺ that can improve diffusion in certain directions, making C₁C_nIm⁺ (with short alkyl chains, $n \leq 4$) good charge carriers in view of their molecular size.⁵⁵ The diffusion of the molecules of 1,3-cyclohexadiene is more than three times faster than the diffusion of the anions in the mixtures and these values increase with increasing concentration of CYD.

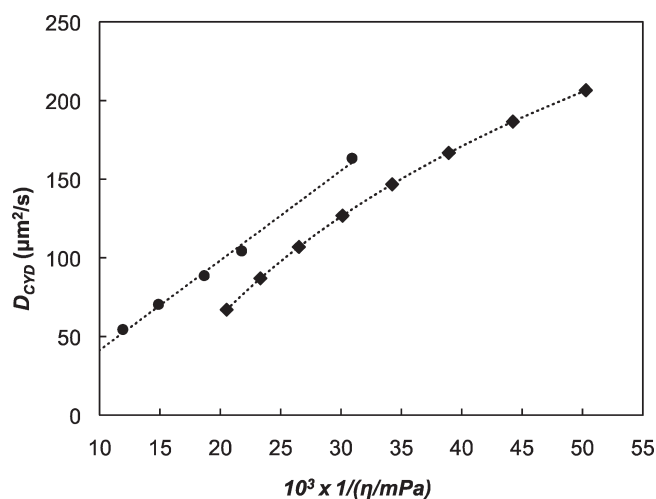


Figure 6. Diffusion coefficients of the 1,3-cyclohexadiene in CYD + [C₁C₄Im][NTf₂] (◆) and CYD + [C₁C₁C₄Im][NTf₂] (●) mixtures as a function reciprocal viscosity of the medium.

According to the Stokes–Einstein equation⁵⁶ the diffusion coefficient of the sphere-like moving species is inversely proportional to the viscosity η of the medium: $D = kT/(f\pi\eta a)$, where k is the Boltzmann constant, f is a constant parameter (equals 6), and a is the radius of the diffusing species. The diffusion coefficient of 1,3-cyclohexadiene in CYD + [C₁C₄Im][NTf₂] and CYD + [C₁C₁C₄Im][NTf₂] mixtures does not follow a linear relationship with reciprocal viscosity (Figure 6), as has been reported by other groups for the diffusion of solutes in imidazolium ionic liquids.³⁵ In some studies, a fractional Stokes–Einstein equation, $D \propto (T/\eta)^\beta$ with $\beta \approx 0.8–0.9$ has been used to describe the relationship between the diffusion and the viscosity.^{57–59}

In continuation of this work, we established the relationship between the diffusion coefficients and the conductivity. From PGSE-NMR self-diffusion coefficients of cations and anions, D_+ and D_- , in [C₁C₄Im][NTf₂] and CYD + [C₁C₄Im][NTf₂] mixtures, conductivity was calculated according to the Nernst–Einstein equation, $\Lambda_{\text{NMR}} = N_A e(D_+ + D_-)/kT$, where N_A is Avogadro's number and e is the electrostatic charge on each ionic carrier. This equation assumes that every diffusing species detected by the NMR measurements contribute to the molar conductivity. In contrast, Λ_{imp} , as described previously, relies on migration of charged species in an electric field.^{50,60} The ratio $\Lambda_{\text{imp}}/\Lambda_{\text{NMR}}$ indicates the proportion of charged species that contribute to the ionic conduction. Thus, $\Lambda_{\text{imp}}/\Lambda_{\text{NMR}}$ is correlated with the ionic nature of ILs and is used as a physicochemical parameter for representing ionicity or dissociation of ILs.

Figure 7 depicts the dependence of the ratio $\Lambda_{\text{imp}}/\Lambda_{\text{NMR}}$ for the CYD+[C₁C₄Im][NTf₂] mixtures including the pure IL. In agreement with other IL systems reported in the literature, it was found that $\Lambda_{\text{imp}}/\Lambda_{\text{NMR}}$ is less than unity, showing the presence of association in ion pairs or larger aggregates, even in the pure IL. The ratio $\Lambda_{\text{imp}}/\Lambda_{\text{NMR}}$ decreases with increasing amount of CYD showing that, although a higher content in organic molecule leads to an increase in diffusion coefficients, it also causes a decrease in the ionicity of the medium, i.e., dilution of the IL in CYD promotes stronger ionic association. This confirms what was already established from the Walden plot (Figure 4). Similar behavior

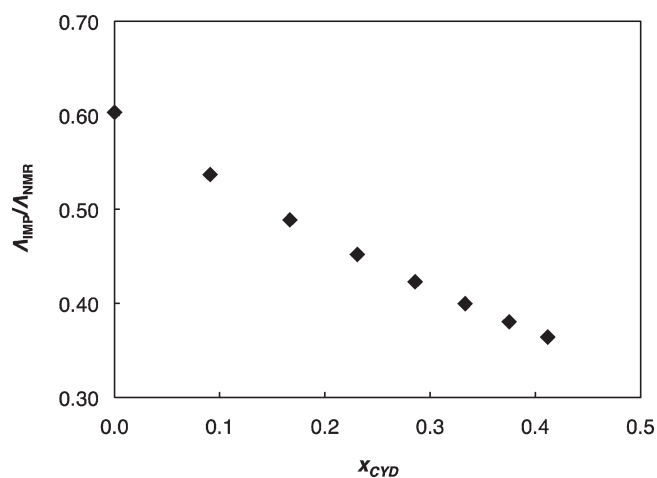


Figure 7. $\Delta_{\text{imp}}/\Delta_{\text{NMR}}$ values for the CYD + $[\text{C}_1\text{C}_4\text{Im}][\text{NTf}_2]$ (\blacklozenge) mixtures as a function of composition.

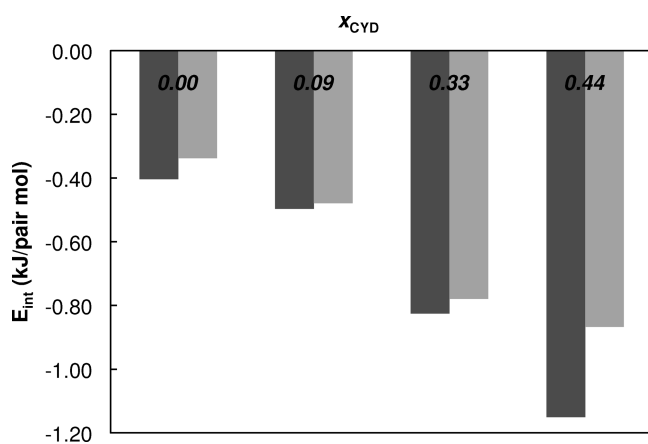


Figure 8. Comparison of the cation–anion interaction energy in the mixtures CYD + $[\text{C}_1\text{C}_4\text{Im}][\text{NTf}_2]$ (dark gray) and CYD + $[\text{C}_1\text{C}_1\text{C}_4\text{Im}][\text{NTf}_2]$ (light gray) at different compositions obtained by molecular simulations. x_{CYD} is molar fraction of 1,3-cyclohexadiene.

was also observed in mixtures of *N,N*-diethyl-*N*-methoxyethynyl-*N*-methylammonium BF_4^- and NTf_2^- with organic solvent such as propylene carbonate or dichloroethane.^{50,60}

Molecular Simulations. Conductivity, viscosity, and diffusion coefficients indicate that addition of CYD to the ionic liquid affects its structure through stronger ionic association. This observation was confirmed also by molecular dynamics simulation, where the overall system configuration energy of the mixtures CYD + IL was decomposed to the energy between each pair of species as represented in Figure 8. The overall cation–anion interactions are stronger for the pair $[\text{C}_1\text{C}_4\text{Im}] + [\text{NTf}_2]$ than for $[\text{C}_1\text{C}_1\text{C}_4\text{Im}] + [\text{NTf}_2]$, which is consistent with the lower ionicity of the former ionic liquid system proved by conductivity and viscosity measurements. It was also observed that, when increasing the amount of CYD present in the mixture, the interaction becomes more negative, confirming again that the addition of molecular solute increases the ion pair association.

NMR. The structural effect of adding CYD to $[\text{C}_1\text{C}_4\text{Im}][\text{NTf}_2]$ and $[\text{C}_1\text{C}_1\text{C}_4\text{Im}][\text{NTf}_2]$ was examined through the change in the chemical shifts of all hydrogen atoms of the ILs (Tables S4

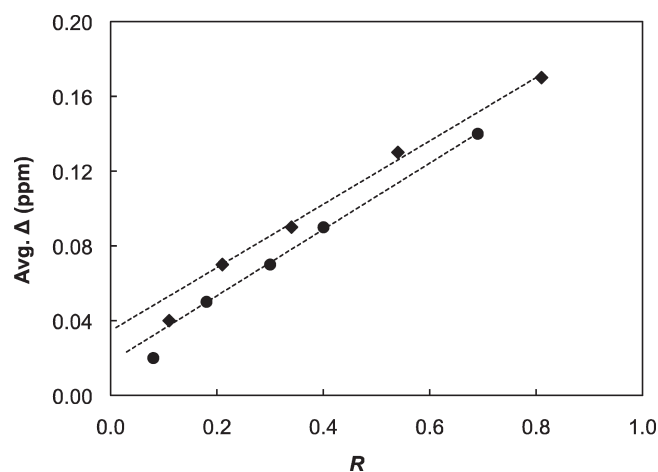


Figure 9. Average deviation of proton chemical shifts in CYD + IL mixtures with respect to pure IL, as a function of composition: CYD + $[\text{C}_1\text{C}_4\text{Im}][\text{NTf}_2]$ (\blacklozenge) and CYD + $[\text{C}_1\text{C}_1\text{C}_4\text{Im}][\text{NTf}_2]$ (\bullet). Note that the first point, corresponding to $R = 0.1$, lies beneath the linear regression in both ILs. So, if the lines exclude the first point of each series, the functions are described as: $\Delta(\text{ppm}) = 0.1694R + 0.0346$ (\blacklozenge) and $\Delta(\text{ppm}) = 0.1773R + 0.0179$ (\bullet).

and S5 in the Supporting Information). The change in the mean chemical shift (relatively to pure ionic liquids), $\Delta\delta$, is plotted with respect to the molar ratio CYD/IL (R) in Figure 9. Atom labeling is depicted in Scheme 2.

All of the chemical shifts of the IL and CYD protons are shifted downfield (Tables S4–S6 in the Supporting Information) contrarily to what we have reported for mixtures of toluene + $[\text{C}_1\text{C}_4\text{Im}][\text{NTf}_2]$ and toluene + $[\text{C}_1\text{C}_1\text{C}_4\text{Im}][\text{NTf}_2]$,³² where all of the chemical shifts of the toluene protons are shifted downfield, whereas the IL protons are shifted upfield when the concentration of organic compound increases. These observations as well as the MD results clearly indicated that the imidazolium cation is found with high probability close to toluene.³² Herein, the evolution of chemical shifts of the IL and CYD protons as well as MD results³⁸ reveal that the preferential solvation sites of the substrate in the ILs are less distinct for CYD than for toluene.

Concerning the proton chemical shifts of ILs (and excluding the first point of each series) $\Delta\delta$ vs mixture composition given by the molar ratio R follows a straight line, as shown in Figure 9. The similar linear variation of the deshielding effect for both ILs was not attributed to a significant structural reorganization, but to the slight changes in the dynamic properties of the system, with increasing CYD concentration, as observed by conductivity measurements.

Catalytic Hydrogenation. We have previously studied the hydrogenation of CYD in $[\text{C}_1\text{C}_4\text{Im}][\text{NTf}_2]$ and $[\text{C}_1\text{C}_1\text{C}_4\text{Im}][\text{NTf}_2]$, at $R = n_{\text{CYD}}/n_{\text{IL}} = 0.5$ using $[\text{Rh}(\text{COD})(\text{PPh}_3)_2][\text{NTf}_2]$ (COD = 1,5-cyclooctadiene) as catalyst.³⁸ Hydrogenation of CYD in both ILs led selectively to cyclohexene (CYE). The fact that the reaction was twice as fast in $[\text{C}_1\text{C}_4\text{Im}][\text{NTf}_2]$ than in $[\text{C}_1\text{C}_1\text{C}_4\text{Im}][\text{NTf}_2]$ could not only be explained in terms of the thermodynamic factors such as CYD solubility or mixing enthalpies of CYD and IL but was related to the ratio of measured viscosities of both ionic liquids studied: $\text{in fact } \eta([\text{C}_1\text{C}_1\text{C}_4\text{Im}][\text{NTf}_2]) / \eta([\text{C}_1\text{C}_4\text{Im}][\text{NTf}_2]) = 1.9$.³⁸

At this point the following question arose: is the relationship between viscosity and reaction rate general for hydrogenation of

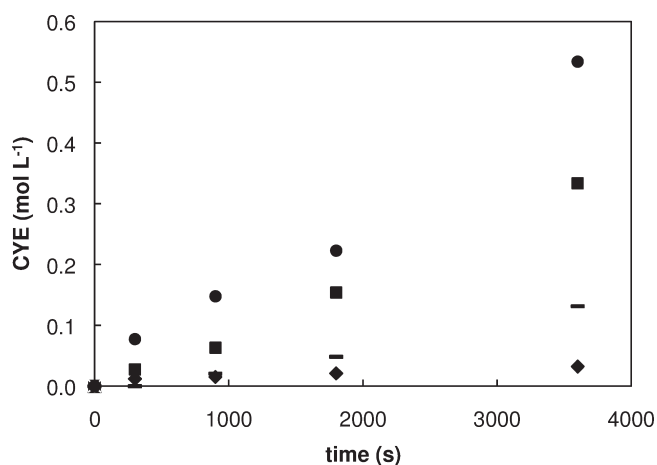


Figure 10. CYE production (mol/L) vs. time (s) in $[C_1C_4Im][NTf_2]$ for $R = 0.2$ (\blacklozenge), 0.3 (—), 0.4 (\blacksquare), and 0.5 (\bullet).

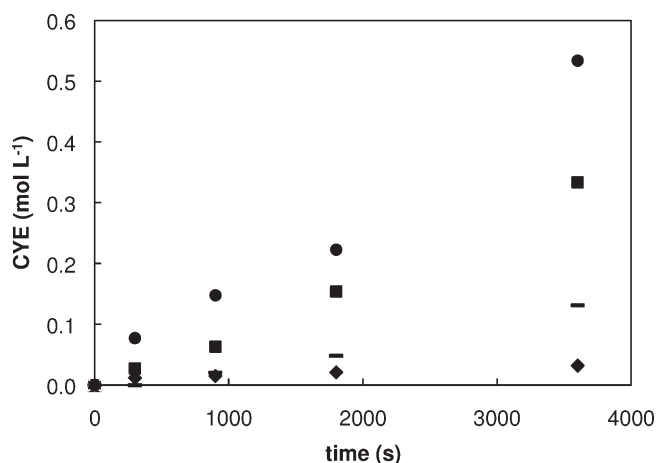


Figure 11. Initial rate ($\text{mol L}^{-1} \text{s}^{-1}$) vs ratio $R = n_{\text{CYD}}/n_{\text{IL}}$ for $[C_1C_4Im][NTf_2]$ (\blacklozenge) and for $[C_1C_1C_4Im][NTf_2]$ (\bullet).

CYD in IL media at all compositions of the reaction mixture? Hence, in this work we report a more in-depth study of the effect of viscosity on the hydrogenation reaction by varying different parameters, such as composition, stirring rate, hydrogen pressure and catalyst loading.

Influence of Composition. All the catalytic reactions were performed at 30°C , under 1.2 bar of hydrogen, and with a molar ratio $n_{\text{CYD}}/n_{\text{catalyst}} = 1000$. Molar ratios $n_{\text{CYD}}/n_{\text{IL}}$, $R = 0.1, 0.2, 0.3, 0.4$, and 0.5 were studied. For all of the systems only CYE was obtained, with the CYE production (mol/L) vs time (s) in $[C_1C_4Im][NTf_2]$ depicted in Figure 10. Reactions with $R > 0.5$ were not performed in order to avoid the formation of a biphasic system due to the low solubility of CYE in IL. In $[C_1C_4Im][NTf_2]$ hydrogenation of CYD at $R = 0.1$ afforded no measurable amount of CYE detected by gas chromatography. With $[C_1C_1C_4Im][NTf_2]$, little to no detectable amount of the hydrogenation product was observed after 1 h of reaction, for all mixtures with $R \leq 0.4$. Data for these experiments are therefore not collected in the Supporting Information in Table S7.

As shown in the Figure 11, the initial rate of hydrogenation in $[C_1C_4Im][NTf_2]$ increases exponentially with the $n_{\text{CYD}}/n_{\text{IL}}$ ratio R , and the rate is not directly proportional to the concentration of

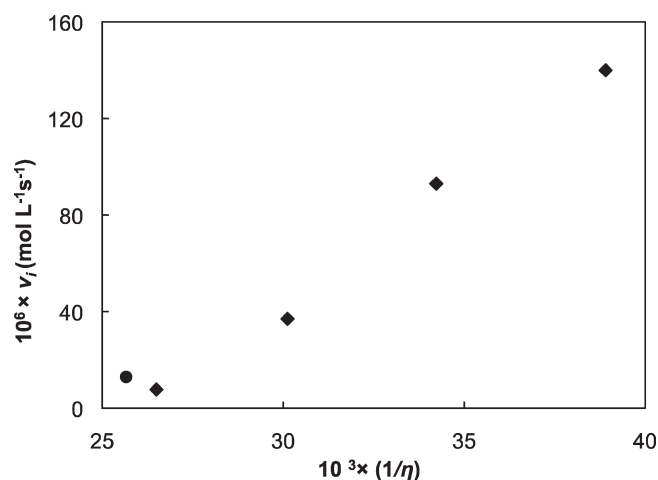


Figure 12. Initial rate ($\text{mol L}^{-1} \text{s}^{-1}$) vs inverse of the viscosity for hydrogenation of CYD in $[C_1C_4Im][NTf_2]$ (\blacklozenge) and $[C_1C_1C_4Im][NTf_2]$ (\bullet). A linear fit of $[C_1C_4Im][NTf_2]$ data (\blacklozenge) gives a straight line with $r^2 > 0.99$.

substrate. Interestingly, when representing initial rates vs inverse of the viscosity, a linear dependence is observed (Figure 12).

The results obtained with $[C_1C_1C_4Im][NTf_2]$ (Figures 11 and 12) are even more interesting. The initial rate observed for $[C_1C_1C_4Im][NTf_2]$ is far from the values obtained for $[C_1C_4Im][NTf_2]$ at the same concentration in CYD (Figure 11), but it is very close to the expected value when viscosity is taken into account (Figure 12). In fact, the initial rate with $[C_1C_1C_4Im][NTf_2]$ represented in Figure 12 is from the mixture at $R = 0.5$ but lies close to the initial rate value obtained with $[C_1C_4Im][NTf_2]$ at $R = 0.2$. Both samples have very different compositions, but quite similar viscosities and H_2 concentrations, meaning that in these systems viscosity is crucial for the catalytic performance. This suggests that the reaction kinetics is controlled by diffusion. In order to see if mass transfer is playing the main role in catalytic hydrogenation of CYD in ILs, hydrogenation experiments with different stirring rates, catalyst loading, and hydrogen pressure were performed.

Effect of Stirring. Two compositions, $R = 0.2$ and 0.5 , were chosen for this experiment (Figure 13a and Table S8 in the Supporting Information). From the results it is clearly seen that increasing the stirring speed leads to a faster reaction regardless of the value R . This shows that mass transfer should be taken into account in the hydrogenation reactions studied here, and that it is important to explain the previous results obtained for $R = 0.2, 0.3, 0.4$, and 0.5 . Note that it has been previously reported that the stirring speed induces also a very strong effect H_2 –ILs mass transfer coefficients.^{61,62}

Effect of H_2 Pressure. Hydrogen is not very soluble in ILs, some authors suggest that the mass transfer of H_2 may limit the rate of olefin hydrogenation processes,^{63,64} whereas others proposed that the high diffusivity of hydrogen results in high hydrogen transfer rates to the catalyst so that, during a hydrogenation reaction, the consumed hydrogen can be replenished rapidly.⁶⁵ In order to determine if this applies to the present system, the reaction was performed under 1.2 and 4 bar of H_2 pressure, at compositions $R = 0.2$ and 0.5 and $n_{\text{CYD}}/n_{\text{catalyst}} = 1000$ (Figure 13b). The production of CYE is dramatically increased under higher pressures of hydrogen, indicating that the pressure under which the reaction is carried out limits the amount of hydrogen in the

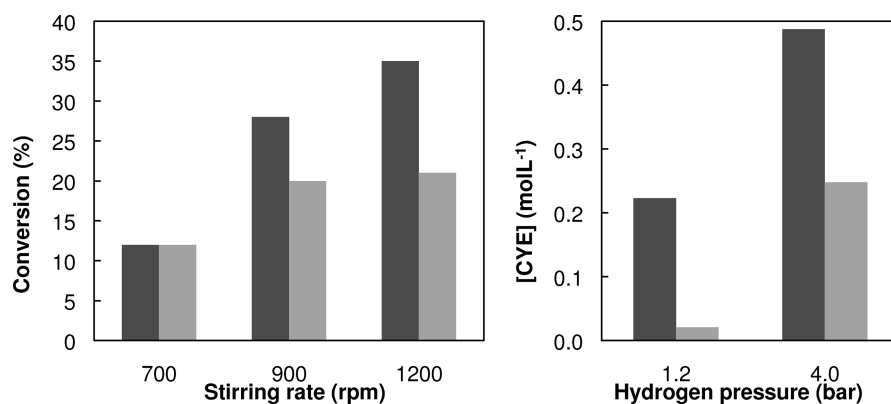


Figure 13. Conversion of CYD into CYE (% , vertical axe) under different stirring rates for compositions: $R = 0.2$ (light gray) and 0.5 (dark gray), left CYE production (mol/L) after 30 min of reaction at compositions $R = 0.2$ (light gray) and $R = 0.5$ (dark gray), under 1.2 and 4 bar of hydrogen, right. The stirring rate was 700 rpm.

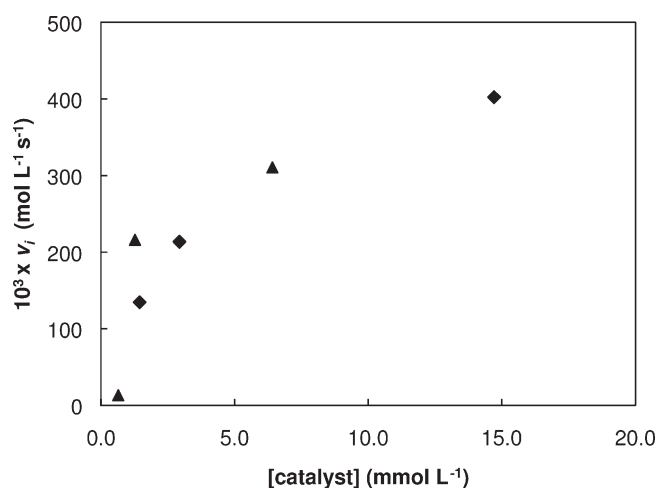


Figure 14. Initial rate (mol L⁻¹ s⁻¹) vs catalyst concentration (mmol L⁻¹) for the hydrogenation of CYD in $[C_1C_4Im][NTf_2]$ at $R = 0.2$ (▲) and 0.5 (◆).

medium. Therefore, H_2 concentration in the medium has to be taken into account as an important rate-determining factor.

Effect of Catalyst Loading. The effect of changing the concentration of catalyst was also studied, at compositions $R = 0.2$ and 0.5 , with $n_{CYD}/n_{catalyst}$ ratios of 100, 500, and 1000. The plot of the measured rates as a function of the initial catalyst concentration is shown in Figure 14. Generally it is accepted that if the reaction is kinetically controlled, i.e., if mass transfer has no effect, then the initial rate should change linearly with catalyst concentration. In particular in the catalytic hydrogenation of dienes as COD (cycloocta-1,5-diene) or NBD (norborna-2,5-diene) with cationic rhodium(I) chelates the pseudorate constant is a linear function of the initial catalyst concentration providing information about the limitations of the regime, which is exclusively controlled by kinetics.^{66–70} In other words, the hydrogen concentration in solution (gas solubility) for the mentioned range of rates is constant, and it is measured in the kinetically controlled range.

This is not the case in the present system as seen in Figure 14, where the reaction rate under the given experimental conditions is determined by mass transport. Because of the rising influence

of diffusion with catalyst concentration, the bulk concentration of hydrogen in solution continuously decreases faster than can be compensated by diffusion. The hydrogenation is slower than would be expected for the kinetically controlled range. These results again support the importance of mass transport.⁷¹

In summary, in the experiments with different values of R described above, it was shown that the initial rate of the catalytic hydrogenation reaction exhibits a linear dependence with the inverse of viscosity. This relationship between the reactivity and the viscosity should be understood in terms of mass transfer issues. In more viscous systems the mobility of molecules is lower and a lower reactivity is observed. The mass transfer issues have been highlighted by investigations of the effect of stirring, catalyst loading and hydrogen pressure.

Mass transport effects in reactions in ILs has been often proposed for catalytic hydrogenation^{4,65,72} and for organic reactions.⁷³ However, to our knowledge, no work before this one has been published concerning the study of all catalytic reaction compositions, carefully calculated in order to keep all parameters constant (including the concentration of hydrogen) except the concentration ratio CYD/IL, allowing us to evidence the prevailing effects of the solvation and mass transfer (viscosity and diffusivity) on the chemical reaction.

CONCLUSIONS

In this work we studied the influence of the nature of two ionic liquids, namely 1-butyl-3-methylimidazolium bis(trifluoromethylsulfonyl)imide, $[C_1C_4Im][NTf_2]$, and 1-butyl-2,3-dimethylimidazolium bis(trifluoromethylsulfonyl)imide, $[C_1C_1C_4Im][NTf_2]$, on the kinetics of the catalytic hydrogenation of 1,3-cyclohexadiene with $[Rh(COD)(PPh_3)_2]NTf_2$ ($COD = 1,5$ -cyclooctadiene). For this purpose, the effect of the concentration of 1,3-cyclohexadiene on the molecular interactions, the structure, and the physicochemical properties in mixtures with the two ionic liquids was investigated. Measurements of the viscosity of 1,3-cyclohexadiene + ionic liquid mixtures at different compositions showed that mixtures with $[C_1C_1C_4Im][NTf_2]$ are more viscous than with $[C_1C_4Im][NTf_2]$, reflecting the order of viscosities of the pure ionic liquids. Furthermore, determination of mass and charge transport properties of the mixtures 1,3-cyclohexadiene + ionic liquid, by DOSY NMR and conductivity measurements, allowed access to the ionicity of the mixtures. It was established that pure

[C₁C₁C₄Im][NTf₂] is more ionic than pure [C₁C₄Im][NTf₂], in agreement with the presence of hydrogen bonds in the latter. From the dependence of the ratio of conductivities obtained by impedance method and NMR ($\Lambda_{\text{imp}}/\Lambda_{\text{NMR}}$) on the concentration of 1,3-cyclohexadiene, it was found that increasing the amount of 1,3-cyclohexadiene leads to a decrease in the ionicity of the media through stronger ionic association. This was confirmed by calculations of the cation–anion pair association energy by molecular dynamics simulations. In spite of this stronger association, conductivity increases when the concentration of 1,3-cyclohexadiene increases, meaning that the effect of the decrease in viscosity, and hence the increase in mobility of charged species, is dominant.

The catalytic hydrogenation of 1,3-cyclohexadiene in [C₁C₄Im][NTf₂] and [C₁C₁C₄Im][NTf₂] yields cyclohexene selectively. The reaction is strongly affected by the viscosity of the medium, and a linear relationship was found between the initial rate of the reaction and the inverse of viscosity. In less viscous systems there is a higher mobility of reactants, so higher conversions and reaction rates are observed. The mass transfer issues were also highlighted by experiments with different catalyst loadings and higher hydrogen pressure.

■ ASSOCIATED CONTENT

S Supporting Information. Density, viscosity, and conductivity data for the mixtures CYD + [C₁C₄Im][NTf₂] and CYD + [C₁C₁C₄Im][NTf₂]; DOSY NMR pulse sequence; diffusion coefficients of cations, anions, and CYD; ¹H NMR shifts; initial rates and conversions for the hydrogenation of CYD in [C₁C₄Im][NTf₂] and [C₁C₁C₄Im][NTf₂]. This material is available free of charge via the Internet at <http://pubs.acs.org>.

■ ACKNOWLEDGMENT

P.C. acknowledges the Ph.D. grant attributed by the Ministère de l'Enseignement Supérieur et de la Recherche, France. G.S and A.P. are financed by the project CALIST of the ANR, France.

■ REFERENCES

- (1) Olivier-Bourbigou, H.; Magna, L.; Morvan, D. *Appl. Catal., A* **2010**, *373*, 1.
- (2) Wasserscheid, P.; Welton, T. *Ionic liquids in synthesis*; Wiley-VCH: Weinheim, Germany, 2008.
- (3) Parvulescu, V. I.; Hardacre, C. *Chem. Rev.* **2007**, *107*, 2615.
- (4) Hallett, J. P.; Welton, T. *Chem. Rev.* **2011**, *111*, 3508.
- (5) Hubbard Colin, D.; Illner, P.; van Eldik, R. *Chem. Soc. Rev.* **2011**, *40*, 272–290.
- (6) Taylor, A. W.; Licence, P.; Abbott, A. P. *Phys. Chem. Chem. Phys.* **2011**, *13*, 10147–10154.
- (7) Castiglione, F.; Moreno, M.; Raos, G.; Famulari, A.; Mele, A.; Appetecchi, G. B.; Passerini, S. *J. Phys. Chem. B* **2009**, *113*, 10750–10759.
- (8) Stark, A. Ionic Liquid Structure-Induced Effects on Organic Reactions. In *Topics in Current Chemistry: Ionic Liquids*; Springer-Verlag: Berlin, 2009.
- (9) Welton, T. In *Multiphase Homogeneous Catalysis*; Cornils, B., et al., Eds.; Wiley-VCH: Weinheim, Germany, 2005; Vol. 2, pp 431–454.
- (10) Olivier-Bourbigou, H.; Vallee, C. In *Multiphase Homogeneous Catalysis*; Cornils, B., et al., Eds.; Wiley-VCH: Weinheim, Germany, 2005; Vol. 2, pp 413–431.
- (11) Mathews, C. J.; Smith, P. J.; Welton, T. *J. Mol. Catal. A* **2004**, *214*, 27.
- (12) Lebel, H.; Janes, M. K.; Charette, A. B.; Nolan, S. P. *J. Am. Chem. Soc.* **2004**, *126*, 5046.
- (13) Nolan, S. P. *N-Heterocyclic Carbenes in Synthesis*; Wiley-VCH: Weinheim, Germany, 2006.
- (14) Magna, L.; Chauvin, Y.; Niccolai, G. P.; Basset, J. M. *Organometallics* **2003**, *22*, 4418.
- (15) Lecocq, V.; Olivier-Bourbigou, H. *Oil Gas Sci. Technol.-Rev. L'Institut Francais Pet.* **2007**, *62*, 761.
- (16) Hintermair, U.; Gutel, T.; Slawin, A. M. Z.; Cole-Hamilton, D. J.; Santini, C. C.; Chauvin, Y. *J. Organomet. Chem.* **2008**, *693*, 2407.
- (17) Welton, T. *Coord. Chem. Rev.* **2004**, *248*, 2459.
- (18) Boon, J. A.; Levisky, J. A.; Pflug, J. L.; Wilkes, J. S. *J. Org. Chem.* **1986**, *51*, 480.
- (19) Dupont, J.; Suarez, P. A. Z. *Phys. Chem. Chem. Phys.* **2006**, *8*, 2441.
- (20) Mele, A.; Romano, G.; Giannone, M.; Ragg, E.; Fronza, G.; Raos, G.; Marcon, V. *Angew. Chem.-Int. Ed.* **2006**, *45*, 1123.
- (21) Mathews, C. J.; Smith, P. J.; Welton, T. *J. Mol. Catal. A* **2004**, *214*, 27.
- (22) Triolo, A.; Russina, O.; Fazio, B.; Appetecchi, G. B.; Carewska, M.; Passerini, S. *J. Chem. Phys.* **2009**, *130*, 164521.
- (23) Fuller, J.; Carlin, R. T.; Delong, H. C.; Haworth, D. *J. Chem. Soc., Chem. Commun.* **1994**, *3*, 299.
- (24) Hardacre, C.; Holbrey, J. D.; McMath, S. E. J.; Bowron, D. T.; Soper, A. K. *J. Chem. Phys.* **2003**, *118*, 273.
- (25) Pott, T.; Meleard, P. *Phys. Chem. Chem. Phys.* **2009**, *11*, 5469–5475.
- (26) Mele, A. *Chim. Oggi.* **2010**, *28*, 48–55.
- (27) Canongia Lopes, J.; Padua, A. A. H. *J. Phys. Chem. B* **2006**, *110*, 3330.
- (28) Wang, Y. T.; Izvekov, S.; Yan, T. Y.; Voth, G. A. *J. Phys. Chem. B* **2006**, *110*, 3564.
- (29) Padua, A. A. H.; Costa Gomes, M. F.; Lopes, J. C. *Acc. Chem. Res.* **2007**, *40*, 1087.
- (30) Canongia Lopes, J. N.; Costa Gomes, M. F.; Padua, A. A. H. *J. Phys. Chem. B* **2006**, *110*, 16816.
- (31) Lachwa, J.; Bento, I.; Duarte, M. T.; Lopes, J. N. C.; Rebelo, L. P. N. *Chem. Commun.* **2006**, *23*, 2445.
- (32) Gutel, T.; Santini, C. C.; Padua, A. A. H.; Fenet, B.; Chauvin, Y.; Canongia Lopes, J. N.; Bayard, F.; Costa Gomes, M. F.; Pensado, A. S. *J. Phys. Chem. B* **2009**, *113*, 170.
- (33) Revelli, A. L.; Mutelet, F.; Jaubert, J. N. *J. Phys. Chem. B* **2010**, *114*, 4600.
- (34) Umecky, T.; Saito, Y.; Matsumoto, H. *J. Phys. Chem. B* **2009**, *113*, 8466.
- (35) Vorotyntsev, M. A.; Zinovyeva, V. A.; Picquet, M. *Electrochim. Acta* **2010**, *55*, S063.
- (36) Hunt, P. A. *J. Phys. Chem. B* **2007**, *111*, 4844.
- (37) Kempter, V.; Kirchner, B. *J. Mol. Struct.* **2010**, *972*, 22.
- (38) Campbell, P. S.; Podgorsek, A.; Gutel, T.; Santini, C. C.; Padua, A. A. H.; Costa Gomes, M. F.; Bayard, F.; Fenet, B.; Chauvin, Y. *J. Phys. Chem. B* **2010**, *114*, 8156.
- (39) Widegren, J. A.; Saurer, E. M.; Marsh, K. N.; Magee, J. W. *J. Chem. Thermodyn.* **2005**, *37*, 569.
- (40) Canongia Lopes, J. N.; Deschamps, J.; Padua, A. A. H. *J. Phys. Chem. B* **2004**, *108*, 2038.
- (41) Canongia Lopes, J. N.; Padua, A. A. H. *J. Phys. Chem. B* **2004**, *108*, 16893.
- (42) Canongia Lopes, J. N.; Shimizu, K.; Padua, A. A. H.; Umabayashi, Y.; Fukuda, S.; Fujii, K.; Ishiguro, S. I. *J. Phys. Chem. B* **2008**, *112*, 9449.
- (43) Jorgensen, W. L.; Maxwell, D. S.; Rives, J. T. *J. Am. Chem. Soc.* **1996**, *118*, 11225.
- (44) Smith, W.; Forester, T. R.; Todorov, I. T. *The DL_POLY molecular simulation package*, 2.20; STFC Daresbury Laboratory: Warrington, U.K., 2007.
- (45) *Transport Properties of Fluids: Their Correlation, Prediction and Estimation*; Cambridge University Press: New York, 2005.

- (46) Mantz, R. A. *Electrochemical Properties of Ionic Liquids*. In *Ionic Liquids in Synthesis*; Wiley-VCH Verlag GmbH & Co: Weinheim, Germany, 2008.
- (47) Walden, P. *Z. Phys. Chem.* **1906**, *55*, 207.
- (48) Angell, C. A.; Byrne, N.; Belieres, J. P. *Acc. Chem. Res.* **2007**, *40*, 1228.
- (49) Yoshizawa, M.; Xu, W.; Angell, C. A. *J. Am. Chem. Soc.* **2003**, *125*, 15411.
- (50) Ueno, K.; Tokuda, H.; Watanabe, M. *Phys. Chem. Chem. Phys.* **2010**, *12*, 1649.
- (51) MacFarlane, D. R.; Forsyth, M.; Izgorodina, E. I.; Abbott, A. P.; Annat, G.; Fraser, K. *Phys. Chem. Chem. Phys.* **2009**, *11*, 4962.
- (52) Fumino, K.; Wulf, A.; Ludwig, R. *Angew. Chem.-Int. Ed.* **2008**, *47*, 8731.
- (53) Tokuda, H.; Tsuzuki, S.; Susan, M.; Hayamizu, K.; Watanabe, M. *J. Phys. Chem. B* **2006**, *110*, 19593.
- (54) Tokuda, H.; Hayamizu, K.; Ishii, K.; Abu Bin Hasan Susan, M.; Watanabe, M. *J. Phys. Chem. B* **2004**, *108*, 16593.
- (55) Kowsari, M. H.; Alavi, S.; Ashrafizaadeh, M.; Najafi, B. *J. Chem. Phys.* **2008**, *129*, 224508.
- (56) Cohen, M. H.; Turnbull, D. *J. Chem. Phys.* **1959**, *31*, 1164.
- (57) Kanakubo, M.; Harris, K. R.; Tsuchihashi, N.; Ibuki, K.; Ueno, M. *J. Phys. Chem. B* **2007**, *111*, 2062.
- (58) Spohr, H. V.; Patey, G. N. *J. Chem. Phys.* **2008**, *129*, 064517.
- (59) Koddermann, T.; Ludwig, R.; Paschek, D. *Chem. Phys. Chem.* **2008**, *9*, 1851.
- (60) Tokuda, H.; Baek, S. J.; Watanabe, M. *Electrochemistry* **2005**, *73*, 620.
- (61) Sharma, A.; Julcour, C.; Kelkar, A. A.; Raj, M.; Deshpande; Delmas, H. *Ind. Eng. Chem. Res.* **2009**, *48*, 4075–4082.
- (62) Morgan, D.; Ferguson, L.; Scovazuzo, P. *Indust. Eng. Chem. Res.* **2005**, *44*, 4815.
- (63) Migowski, P.; Zanchet, D.; Machado, G.; Gelesky, M. A.; Teixeira, S. R.; Dupont, J. *Phys. Chem. Chem. Phys.* **2010**, *12*, 6826.
- (64) Dyson, P. J.; Laurenczy, G.; Ohlin, C. A.; Vallance, J.; Welton, T. *Chem. Commun.* **2003**, 2418–2419.
- (65) Wasserscheid, P.; Schulz, P. *Handbook of homogeneous hydro-generation*; de Vries, J. G., Elsevier, C. J., Eds.; Wiley-VCH V: Weinheim, Germany, 2007; Vol. 1, Chapter 41, p 1389.
- (66) Vincent, T.; Guibal, E. *Langmuir* **2003**, *19*, 8475.
- (67) Khilnani, V. L.; Chandalia, S. B. *Org. Process Res. Dev.* **2001**, *5*, 263.
- (68) Rode, C. V.; Vaidya, M. J.; Jaganathan, R.; Chaudhari, R. V. *Chem. Eng. Sci.* **2001**, *56*, 1299.
- (69) Rajashekharan, M. V.; Bergault, I.; Fouilloux, P.; Schweich, D.; Delmas, H.; Chaudhari, R. V. *Catal. Today* **1999**, *48*, 83.
- (70) Galvagno, S.; Capannelli, G.; Neri, G.; Donato, A.; Pietropaolo, R. *J. Mol. Catal.* **1991**, *64*, 237.
- (71) Drexler, H.-J.; Preetz, A.; Schmidt, T.; Heller, D. In *Handbook of homogeneous catalysis*; de Vries, J. G., Elsevier, C. J., Eds.; Wiley-VCH V: Weinheim, Germany, 2007; Vol. 1, Chapter 41, p 257.
- (72) Hardacre, C.; Mullan, C.; Rooney, D. W.; Thompson, J. M.; Yablonsky, G. S. *Chem. Eng. Sci.* **2006**, *61*, 6995–7006.
- (73) Chiappe, C. *Ionic Liquids in Organic Synthesis: Effects on Rate and Selectivity*. In *Ionic Liquids in Synthesis*; Wiley-VCH Verlag GmbH & Co. KGaA: Weinheim, Germany, 2004.